Suppression of the quantum fluctuation in ^{18}O-enriched strontium titanate

Ruiping Wang* and Mitsuru Itoh†
Materials & Structures Laboratory, Tokyo Institute of Technology, 4259 Nagatsuta, Midori, Yokohama 226-8503, Japan
(Received 19 May 2001; published 3 October 2001)

The dielectric properties of structurally monodomain, oxygen-isotope-exchanged $SrTiO_3$ samples, $SrTi(^{16}O_{1-x}\ ^{18}O_x)_3$, were investigated. It was found that ferroelectricity is intrinsic to $SrTi(^{16}O_{1-x}\ ^{18}O_x)_3$ ($x \geqslant 0.33$), and that twin boundaries do not affect their overall dielectric behaviors. Quantitative analyses reveal that the replacement of ^{16}O with ^{18}O mainly suppresses the quantum fluctuation in $SrTiO_3$, and leaves the ferroelectric fluctuation nearly unchanged.

DOI: 10.1103/PhysRevB.64.174104 PACS number(s): 77.22.Ch, 77.22.Ej, 77.80.Bh

I. INTRODUCTION

The current trend in electronic products, such as mobile phones and portable computers, is miniaturization, which demands smaller-sized components for a given capacitance. Therefore, the development of new dielectric materials with a high dielectric constant is in practical demand. Recently, another ferroelectric, oxygen-isotope-exchanged $SrTiO_3$, $SrTi(^{16}O_{1-x}\ ^{18}O_x)_3$, was discovered by the present authors' group[1] A dielectric constant value of 172000, which is the highest dielectric value among the classical and quantum oxide ferroelectrics, was reached at $\sim$3.1 K by a $x=0.37$ oxygen-isotope-exchanged $SrTiO_3$,[2] signifying the potential application of $SrTi(^{16}O_{1-x}\ ^{18}O_x)_3$ at cryogenic temperatures.

The evolution of the ferroelectricity in $SrTi(^{16}O_{1-x}\ ^{18}O_x)_3$ with oxygen-isotope exchange rate $x \geqslant 0.33$ has been demonstrated by dielectric constant, pyroelectricity, *DE*-loop measurements, and so on.[1,2] Recently, Brillouin scattering,[3] Raman scattering,[4] and birefringence[5] measurements, etc. have further confirmed the ferroelectric phase transition in $SrTi(^{16}O_{1-x}\ ^{18}O_x)_3$ ($x \geqslant 0.33$). The strong dependence of the real part of the dielectric constant on the amplitude of the test signal and the relaxation of the remnant polarization discriminate the low-temperature state from that of the prototype ferroelectric $BaTiO_3$. We have suggested that the low-temperature state of $SrTi(^{16}O_{1-x}\ ^{18}O_x)_3$ is a random field-induced domain state.[6] The evolution of ferroelectricity in $SrTi(^{16}O_{1-x}\ ^{18}O_x)_3$ has been proposed to be closely related to the contest between the quantum fluctuation and the ferroelectric fluctuation.[6] High pressure depresses both the ferroelectric phase transition temperature and the dielectric constant, revealing that the system probably belongs to the displacive type ferroelectrics.[7] The dielectric properties of $SrTi(^{16}O_{1-x}\ ^{18}O_x)_3$ have been investigated on [100]-oriented samples. For such an orientation, below the zone-boundary transition ($T_a=105$ K),[8] the rotation of the TiO_6 octahedra around the pseudocubic [100] directions will produce a twin boundary and influence the dielectric properties. To quantitatively discuss the dielectric properties of the $SrTiO_3$-based samples, monodomain (that is, twin-boundary free) crystals are necessary. Müller *et al.* reported that a monodomain sample could be obtained by cutting crystals parallel to the twin-boundary plane (110) with a special geometry.[9]

In the present paper, monodomain ^{18}O-isotope-exchanged samples were prepared and their dielectric properties were studied. It was found that the ferroelectricity of monodomain $SrTi(^{16}O_{1-x}\ ^{18}O_x)_3$ samples is qualitatively the same as that of multidomain samples. Quantitative analyses revealed that the substitution of ^{16}O with its heavy isotope ^{18}O mainly suppresses the quantum fluctuation in $SrTiO_3$, and leaves the ferroelectric fluctuation nearly unchanged.

II. EXPERIMENT

Single crystal plates of $SrTiO_3$ were cut with edges parallel to the twin-boundary plane (110) and geometries $\sim 7 \times 3 \times 0.7\ mm^3$ (Fig. 1) from a single crystal lump. They were polished to optical quality then etched in boiling orthophosphoric acid for about 3 h to remove the stressed surface layers.[10] The final sizes of the crystals were about $7 \times 3 \times 0.3\ mm^3$. Oxygen-isotope exchange was carried out by heating the plates at 1323 K in $^{18}O_2$ gas (Isotech Co.). The exchange rate, *x*, was determined from the weight increment of the crystals. Seven samples, with exchange rates of 0% (STO 16), 25%(STO 18-25), 38%(STO 18-38), 45%(STO 18-45), 60%(STO 18-60), 75%(STO 18-75), and 84%(STO 18-84), respectively, were obtained. The homogeneous distribution of the ^{18}O was ensured by vacuum annealing the samples (except STO 16) at 1323 K for 500 h.

Gold paste, burnt onto the large faces of the samples at 873 K, served as electrodes. The complex dielectric constant (ε) of the samples was measured in the frequency range of $20\ Hz \leqslant f \leqslant 1$ MHz and the temperature range of $2.2\ K < T < 300$ K by using an HP4284A LCR meter. To avoid nonlin-

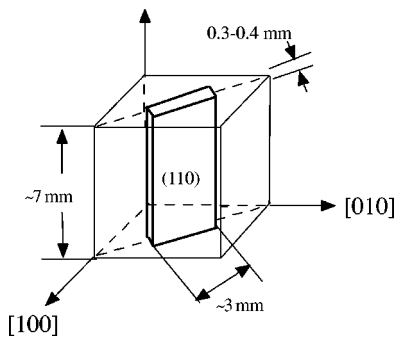

FIG. 1. Orientation and geometry of crystals.

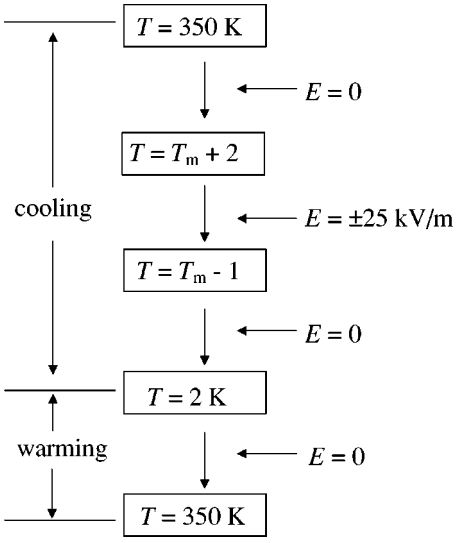

FIG. 2. Flow chart for the pyroelectricity measurement.

ear contribution, a low amplitude (E_0) of the ac test signal, $E_0 = 0.04$ kV/m, was used. Pyroelectricity (P) of the samples was measured by using a homemade apparatus and a Keithley 6517 electrometer/high resistance meter. The flowchart for pyroelectricity measurement is shown in Fig. 2. The sample was zero-field cooled from 350 K at a rate of 3 K/min to just above the phase transition temperature T_c, then poling was carried out by applying an electric field ± 25 kV/m in the temperature range of $T_c - 1 < T < T_c + 2$ K during cooling. After the sample had been cooled to 2 K, it was heated at a rate of 3 K/min under zero fields and the pyroelectricity data was recorded during the warming run. No effort to saturate the polarization was attempted. Relaxation of remnant polarization (P) at temperature $T(<T_c)$ was measured by slow-cooling the sample in a poling field E from ~350 K to T, then switching off E and recording P for periods up to $t = 10^3$ s, by using a Keithley 6517 electrometer/high resistance meter.

III. RESULTS AND DISCUSSION

Figures 3 and 4 show variation of the real part (ε') and the imaginary part (ε'') of the dielectric constant with temperature ($2.2\,\mathrm{K} < T < 50\,\mathrm{K}$) at a frequency $f = 10$ kHz for all of the samples, respectively. ε' of STO16 increases with decreasing T monotonically, and becomes almost temperature-independent at $T < 10$ K, showing the typical quantum paraelectric behavior. The fitting of ε' vs T data in the temperature range of $30\,\mathrm{K} < T < 100\,\mathrm{K}$ to the Barrett formula

$$\varepsilon = \frac{M}{(T_1/2)\coth(T_1/2T) - T_0} \tag{1}$$

gives the best-fit parameters $M = 1.06 \times 10^5$, $T_1 = 87$ K, and $T_0 = 36$ K, which are in good agreement with findings in a previous report.[11] A low dielectric loss is detected for this sample, verifying the good quality of the sample and the reliability of the measurement. A small amount of

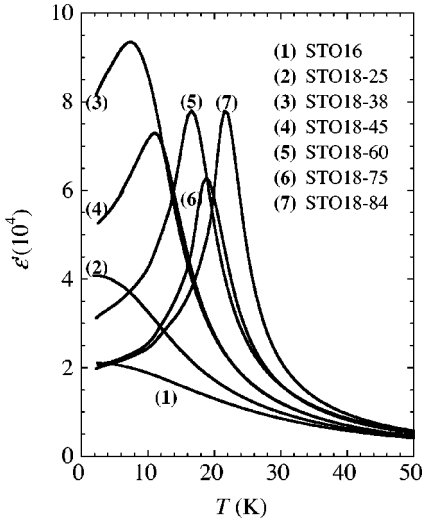

FIG. 3. The real part of the dielectric constant measured at $f = 10$ kHz.

^{18}O-isotope exchange ($x \leqslant 0.25$) does not change the overall quantum paraelectric behavior, though the ε' value is strongly enhanced due to the ^{18}O-isotope-exchange-induced softening of the lattice.[2] On further increasing the exchange rate, both ε' and ε'' show peak at low temperatures. The ε' peak is rounded for low x samples, and its half-width decreases with increasing x. A maximum peak value $\varepsilon' = 94\,000$ was observed for the $x = 0.38$ sample at a frequency $f = 10$ kHz. Coincident with the appearance of the ε' and ε'' peak, a spontaneous polarization (P) is observed for samples with $x > 0.25$ (Fig. 5). P is nonzero at low temperatures. With increasing temperature to slightly lower than the dielectric constant peak temperature T_m, P begins to decrease and the decreasing rate reaches a maximum around T_m. When the polarizing field is reversed, a reversal of P in the samples is clearly observed (data not shown here). The observation of P at $T < T_m$ and the disappearance of P at $T > T_m$ are evidence

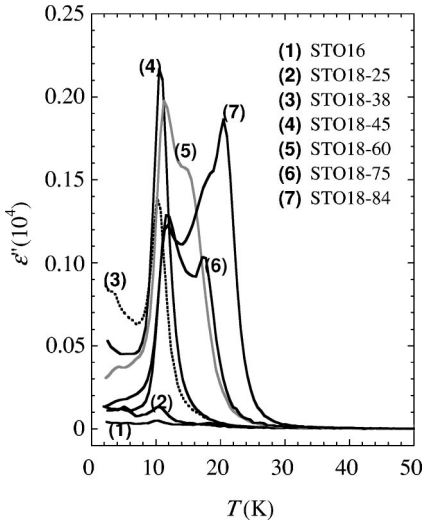

FIG. 4. The imaginary part of the dielectric constant measured at $f = 10$ kHz.

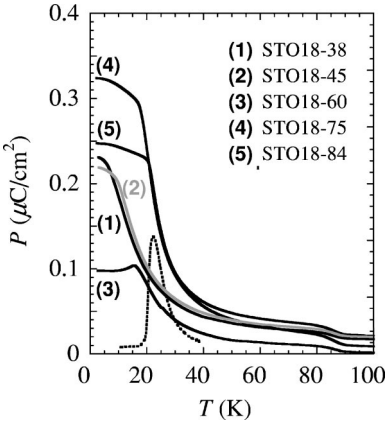

FIG. 5. Variation of the spontaneous polarization with temperature. The poling field is 25 kV/m. The broken line shows dP/dT versus T for STO18-84.

that (1) the ferroelectric interaction evolves at low temperatures for samples with $x>0.25$; and (2) the ε' and ε'' peaks result from a ferroelectric phase transition and T_m corresponds to the ferroelectric phase transition temperature T_c.

Similar to the case for the multidomain samples,[2] in the monodomain samples the phase transition temperature T_c shifts to a high temperature with x in a nonlinear manner [Fig. 6(a)]. The application of the quantum ferroelectric

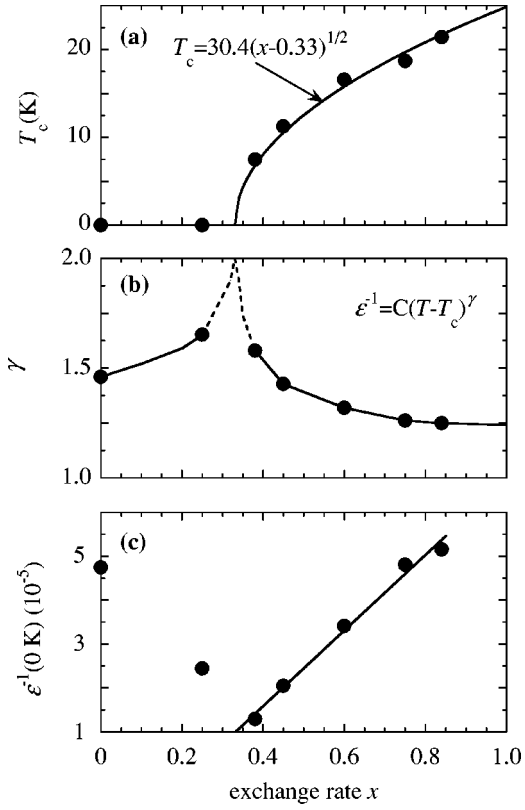

FIG. 6. The exchange rate x dependence of (a) the transition temperature T_c, (b) the critical exponent γ, and (c) the inverse dielectric constant at 0 K. The solid lines are the best fit to the quantum ferroelectric relations (see text), and the broken lines in (b) show our assumption.

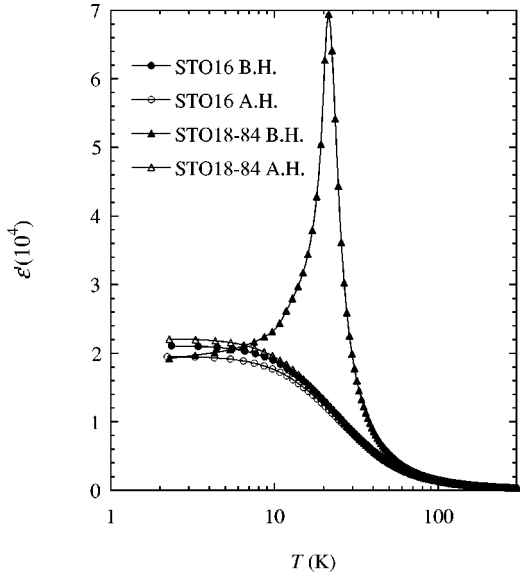

FIG. 7. The real part of the dielectric constant for STO16 and STO18-84 before and after the long-term heating in flowing $^{16}O_2$ gas. B.H.: before heating; A.H.: after heating.

formula[12]

$$T_c = A(x - x_c)^{1/2} \tag{2}$$

to the data shown in Fig. 6(a) gives a reasonable fit with the best-fit parameters $A=30.4$ and a critical composition $x_c=0.33$. The critical exponent γ, which is obtained by fitting ε' data on the high temperature side of $T_c(T_c+25\,\mathrm{K}<T<T_c+50\,\mathrm{K})$ to the formula

$$1/\varepsilon' = C(T - T_c)^{\gamma} \tag{3}$$

is shown in Fig. 6(b). While x_c is approached, either from the low or the high x side of x_c, γ increases strongly, showing a tendency to approach the theoretical value, $\gamma=2$, for a quantum ferroelectric with $x=x_c$. In Fig. 6(c), the inverse dielectric constant at 0 K, $\varepsilon^{-1}(0\,\mathrm{K})$, is plotted as a function of the exchange rate x. $\varepsilon^{-1}(0\,\mathrm{K})$ at $x>x_c$ varies linearly with x. The solid line shows the best-fit curve to the quantum ferroelectric relation[12]

$$\varepsilon^{-1}(0\ \mathrm{K}) \propto x - x_c \tag{4}$$

at $x>x_c$. The reasonable fitting of T_c, γ, and $\varepsilon^{-1}(0\,\mathrm{K})$ to the quantum ferroelectric relations supports our previous conclusion that the $SrTi(^{16}O_{1-x}\ ^{18}O_x)_3$ with $x \geqslant 0.33$ are quantum ferroelectrics.[2]

To identify the origin of the ferroelectricity of the $SrTi(^{16}O_{1-x}\ ^{18}O_x)_3$ samples, two experiments were performed. First, the STO16 sample was heated in flowing $^{16}O_2$ gas for a period of time longer than 500 h. Second, reverse exchange was carried out for the STO 18-84 sample by heating the sample in flowing $^{16}O_2$ gas for a long time until $x \sim 0$ verified via weight decrement of the crystal. In Fig. 7, ε' values for the two samples before and after the heating in $^{16}O_2$ gas are comparatively shown. From the figure, the following two points are apparent: (1) the quantum paraelectric behavior of STO16 was not changed; that is, no ferroelec-

TABLE I. T_c and the best-fit parameters to Eq. (1).

	T_c (K)	$M(10^5)$	T_1 (K)	T_0 (K)	T_1-2T_0 (K)
STO16		1.06±0.01	87±1	36±1	11
STO18–25		1.06±0.01	84±1	37±1	10
STO18–38	7.4	1.05±0.02	79±1	37±1	5
STO18–45	11.3	1.05±0.02	80±1	37±1	6
STO18–60	16.6	1.21±0.02	76±1	37±1	2
STO18–75	18.7	1.12±0.02	74±1	37±1	0
STO18–84	21.4	1.18±0.02	71±1	37±1	−3

tricity was induced in STO16 by the long-term heating in $^{16}O_2$ gas; and (2) the ferroelectricity of STO18-84 vanished and the quantum paraelectric behavior was restored after the reverse exchange. The above results clearly show that the ferroelectricity of the $SrTi(^{16}O_{1-x}\ ^{18}O_x)_3$ samples is induced via replacing ^{16}O with ^{18}O in $SrTiO_3$.

For all seven samples, ε' data within the temperature range of $30\ K<T<100\ K$ can be satisfactorily fit to the Barrett formula (1) with the best-fit parameters listed in Table I. T_0, which indicates the Curie-Weiss temperature, is almost exchange rate x independent, whereas T_1, which is the dividing point between the low temperature region where quantum effects are important and the high temperature region where a classical approximation is good, shows a tendency of decreasing with x. The results intimate that oxygen-isotope exchange mainly suppresses the quantum fluctuation in STO16 and leaves the ferroelectric fluctuation nearly unaffected. STO16 at low temperature is at a critical state; that is, the ferroelectric fluctuation is barely suppressed by the quantum fluctuation. Therefore, even a subtle change between the two fluctuations could induce a drastic change: from a quantum paraelectric to a quantum ferroelectric. Actually, T_1-$2T_0$, which can be considered as a rough measurement of the competition between the quantum fluctuation and the ferroelectric fluctuation, decreases continuously with x, from 11 for STO16 to 0 for STO 18-75, and finally becomes negative for STO 18-84, indicating that the ferroelectric fluctuation becomes stronger than the quantum fluctuation in this sample. The gradual decrease of T_1-$2T_0$ indicates that the balance between the two fluctuations is changed gradually. While the exchange rate x is low ($x<x_c$), the ferroelectric fluctuation is still weaker than the quantum fluctuation; the formation of the ordered state at low temperatures is obstructed, and the effects of the ^{18}O-isotope exchange manifest only as a higher ε'. On increasing x further, the ferroelectric fluctuation becomes stronger due to the continuous weakening of the quantum fluctuation, and the ordered state is achieved. However, the fact that the T_c of the STO18-84 sample still follows the quantum ferroelectric relation (2) clearly suggests that the quantum fluctuation is not negligible, even for a sample with such a high exchange rate.

If the force constant is not changed via replacement of ^{16}O with ^{18}O, according to quantum mechanics, the zero-point energy (that is the quantum fluctuation) is proportional to $\mu^{-1/2}$, where μ represents the reduced mass of the relevant vibrating system. On replacement of ^{16}O with ^{18}O, μ increases. For example, $(\mu_{18}/\mu_{16})^{-1/2}$ for the Slater mode is calculated to be ~1.03. That is, the quantum fluctuation is suppressed via the oxygen-isotope exchange in $SrTiO_3$. This is in consistent with the results in the Table I, further confirming that mass is one of the factors determining the ferroelectric transitions in the perovskite oxides, and that the evolution of the ferroelectricity in $SrTi(^{16}O_{1-x}\ ^{18}O_x)_3$ is mainly due to the lattice stabilization by the heavy atoms. Hidaka *et al.*investigated the effects of cation isotopic exchange on the ferroelectric phase transition temperature T_c of $BaTiO_3$.[13] In their study, reverse results were obtained: T_c of $BaTiO_3$ was shifted to high temperature by introducing lighter isotopes and to low temperature by introducing heavier isotopes. No explanation has been given to the cation isotope exchange-induced phenomena in $BaTiO_3$.

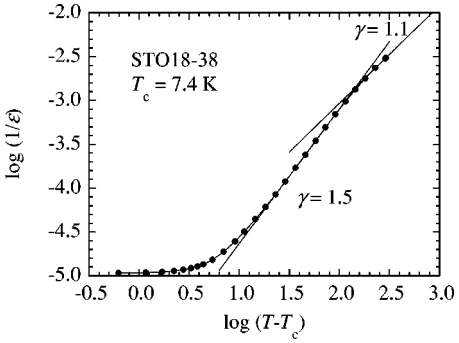

FIG. 8. Log $(1/\varepsilon')$ versus $\log(T-T_c)$ for STO18-38. The critical exponent γ shows crossover from 1.5 at low temperatures to 1.1 at high temperatures.

The opposite effects of the cation and anion isotopic exchange on the ferroelectric phase transition temperature of the perovskite oxide clearly indicate that cation and anion contribute to the ferroelectric phase transition of the perovskite oxide in different ways. The introduction of isotopes has several effects: mass effect, volume effect, and so on. Usually, the mass effect predominates, as in the case of $SrTi(^{16}O_{1-x}\ ^{18}O_x)_3$. However, the reverse effects of the cation isotopic exchange on T_c of $BaTiO_3$ may suggest that volume effect plays a significant role when the cation isotopes are concerned. T_1-2T_0 has been taken as a rough measurement of the competition between the quantum fluctuation and the ferroelectric fluctuation.[1,14] $T_1-2T_0=0$ means that the quantum fluctuation is completely compensated by the ferroelectric fluctuation. Thus, it is expectable that the oxygen isotope exchange rate $x(T_1-2T_0=0)$ should be in coincident with the critical exchange rate x_c. However, in the present study, $x(T_1-2T_0=0)$ $(=0.75)$ differs from $x_c(=0.33)$ by a large value. The Barrett formula is a quantum mechanical extension of the mean-field theory of Slater relation, thus not a rigorous one. It has a trend of overestimate T_1 (underestimate T_0) when applied to single crystal $SrTiO_3$.[11] As a result, T_1-2T_0 is shifted to a larger value. We think that the overestimate of T_1 (underestimate T_0) is the main reason that causes $x(T_1-2T_0=0)>x_c$.

Similar to the case for $KTa_{1-x}Nb_xO_3$,[15] a crossover from Barrett to critical behavior was observed. In Fig. 8, the inverse dielectric constant $1/\varepsilon'$ versus $T-T_c$ on a log-log

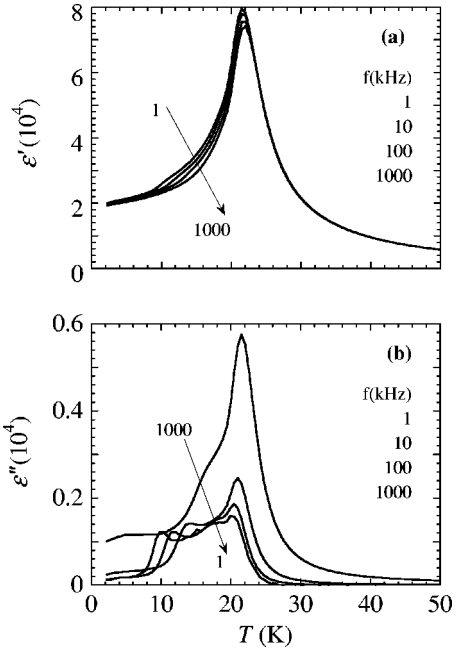

FIG. 9. The (a) real and (b) imaginary part of the dielectric constant for STO18-84 measured under several frequencies. The frequency dispersion is evident.

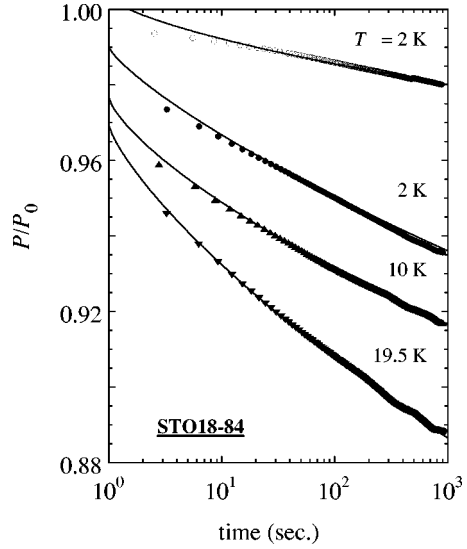

FIG. 10. Normalized remnant polarization P versus time t for STO18-84. The poling field is $E=10$ kV/m for $T=2$ K (●), 10 K (▼), 19.5 K (▲), and 20 kV/m for $T=2$ K (○).

scale of the STO18−38 sample is plotted. In the vicinity of T_c, no critical exponent γ can be evaluated because of the severe rounding at low temperatures. Above $T-T_c\sim 18$ K, the slope becomes constant, indicating that an exponent $\gamma=1.5$. At $T-T_c\sim 100$ K, a deviation from Barrett is observed, and at $T-T_c\sim 140$ K, a crossover to $\gamma=1.1$ takes place. These results further suggest that the quantum fluctuation plays an important role even at low temperatures.

Figures 9(a) and 9(b) show ε' and ε'' for STO18−84 measured under several frequencies. Unlike the typical ferroelectrics $BaTiO_3$,$PbTiO_3$, etc., the peak temperature of STO18−84 shows frequency dispersion, from 22.0 K at $f=1$ MHz to 21.5 K at $f=1$ kHz. Similar dispersion has been observed in solid solutions such as $K_{1-x}Li_xTaO_3$, $Sr_{1-x}Ca_xTiO_3$, and $KTa_{1-x}Nb_xO_3$.[16] Significantly some disorders exist in the system.

To identify the origin of the disorders in $SrTi(^{16}O_{1-x}{}^{18}O_x)_3$, the variation of the remnant polarization P_r with time t was measured after a slow field-cooling process. Figure 10 shows relaxation of the normalized remnant polarization measured under different temperatures and poling fields E for STO18−84. A long-term nonexponential relaxation is observed after the poling field is switched off, and the relaxation shows the following characteristics: (1) for the same poling field $E=10$ kV/m, the rate of relaxation increases with increasing $T(<T_c)$, and P_r decreases by ~5.5% at $T=2$ K and ~8.2% at $T=19.5$ K; (2) for the same temperature $T=2$ K, the rate of relaxation decreases with increasing the poling field, and P_r decreases by ~5.5% at $E=10$ kV/m and ~2.5% at $E=20$ kV/m; (3) the relaxation rate is lower for monodomain samples than for multidomain samples, for the same poling field $E=10$ kV/m and the equivalent temperature $T=T_c-2$ K, and P_r decreases by ~8.2% for the monodomain sample STO18−84 and by ~14% for the ~93% ^{18}O-exchanged multidomain sample STO18.[6] The data in Fig. 10 have been analyzed using several models. Compared to logarithmic, stretched-exponential or simple power laws, the data are best fit by generalized power law[17]

$$P_r/P_0=A\exp\{-\alpha[\ln(t/\tau)]^{\phi}\},\quad t\geqslant\tau. \tag{5}$$

The solid lines in Fig. 10 represent the best-fit results, and the best-fit parameters are listed in Table II. The increase of the exponential α and the decrease of the characteristic relaxation time τ with temperature under 10 kV/m poling field reflect the acceleration of the decay with increasing temperature. When the poling field is increased to 20 kV/m, the decrease of α and increase of τ are observed, demonstrating the field-enhanced ferroelectric interaction between the domains. The exponent ϕ, which is approximately 0.9 for $T=2$ and 10 K, increases to 1.01 for $T=19.5$ K. Apparently, the relaxation behavior of P_r crosses over from the generalized to the simple power law on increasing temperature approaching T_c.

The well fitting of the generalized power law to the data in Fig. 10 indicates that the $SrTi(^{16}O_{1-x}{}^{18}O_x)_3$ is a system with quenched random-field disorder.[17] This result together with the fact that, similar to the case for multidomain samples, a strong nonlinear dependence of the dielectric con-

TABLE II. Best-fit parameters to Eq. (5).

T (K)	E (kV/m)	α	τ (sec)	ϕ
2	10	0.0089	0.11	0.93
10	10	0.0096	0.03	0.91
19.5	10	0.0103	0.01	1.01
2	20	0.0016	0.57	1.18

stant on the amplitude of the ac test signal is observed for the present monodomain samples[18] signify that the low-temperature state of the monodomain $SrTi(^{16}O_{1-x}{}^{18}O_x)_3$ is a random field-induced domain state. Different from the case of *A* site substituted $SrTiO_3$ and $KTaO_3$, in which the random fields mainly come from random dipole and/or random strain fields; the random fields in $SrTi(^{16}O_{1-x}{}^{18}O_x)_3$ probably have the following sources: (1) the extrinsic oxygen vacancies; (2) the competing of the Ti-^{16}O interaction (paraelectriclike) with the Ti-^{18}O interaction (ferroelectriclike). In addition, the relaxation rate of the monodomain samples is slower than that of the multidomain samples and the twin boundaries formed at the zone-boundary phase transition around 105 K (Ref. 8) also appear to be a source of the random fields in $SrTi(^{16}O_{1-x}{}^{18}O_x)_3$.

IV. CONCLUSIONS

The oxygen-isotope exchange-induced quantum ferroelectricity in $SrTi(^{16}O_{1-x}{}^{18}O_x)_3$ was further verified by investigating the dielectric constant and spontaneous polarization of the structural monodomain (twin boundary-free) samples. The origin of the ferroelectricity of the $SrTi(^{16}O_{1-x}{}^{18}O_x)_3$ samples has been identified to be the replacement of ^{16}O by ^{18}O in $SrTiO_3$. The observation of frequency dispersion, the long-term nonexponential relaxation of the remnent polarization, and so on suggests that the low-temperature state of the $SrTi(^{16}O_{1-x}{}^{18}O_x)_3$ is a random field-induced domain state. In addition to extrinsic oxygen vacancies and the competing of the Ti-^{16}O interaction with the Ti-^{18}O interaction, the twin boundaries also form random fields. Thus, it is reasonable to conjecture that, rather than showing the domain state at low temperatures, a monodomain $SrTiO_3$ single crystal with 100% of an oxygen-isotope exchange rate *x*, negligible defects and vacancies should show a ferroelectric with a true long-range order at $T<T_c$.

ACKNOWLEDGMENTS

Part of this work was financially supported by the JSPS research for the Future Program in the Area of Atomic-Scale Surface and Interface Dynamics, and by a Grant-in-Aid for Scientific Research from the Ministry of Education, Science and Culture of Japan.

*Present address: Smart Structure Research Center, National Institute of Advanced Industrial Science and Technology, Tsukuba Central 2, 1-1-1 Umezono, Tsukuba 305-8568, Japan.

†Author to whom correspondence should be addressed. Email address: m.itoh@rlem.titech.ac.jp

[1] M. Itoh, R. Wang, Y. Inaguma, T. Yamaguchi, Y.-J. Shan, and T. Nakamura, Phys. Rev. Lett. **82**, 3540 (1999).

[2] M. Itoh and R. Wang, Appl. Phys. Lett. **76**, 221 (2000).

[3] M. Yamaguchi, T. Yagi, R. Wang, and M. Itoh, Phys. Rev. B **63**, 172102 (2001).

[4] M. Kasahara, H. Hasebe, R. Wang, M. Itoh, and T. Yagi, J. Phys. Soc. Jpn. **70**, 648 (2001).

[5] Kiyoko Yamanaka, Ruiping Wang, Mitsuru Itoh, and Katsunori Iio (unpublished).

[6] R. Wang and M. Itoh, Phys. Rev. B **62**, R731 (2000).

[7] R. Wang, N. Sakamoto, and M. Itoh, Phys. Rev. B **62**, R3577 (2000).

[8] F. W. Lytle, J. Appl. Phys. **35**, 2212 (1964).

[9] K. A. Müller and W. Berlinger, Solid State Commun. **8**, 549 (1970).

[10] K. Aso, Jpn. J. Appl. Phys. **15**, 1243 (1976).

[11] K. A. Müller and H. Burkard, Phys. Rev. B **19**, 3593 (1979).

[12] R. Morf, T. Schneider, and E. Stoll, Phys. Rev. B **16**, 462 (1977).

[13] T. Hidaka and K. Oka, Phys. Rev. B **35**, 8502 (1987).

[14] U. Bianchi, J. Dec, W. Kleemann, and J. G. Bednorz, Phys. Rev. B **51**, 8737 (1995).

[15] R. Kind and K. A. Muller, Commun. Phys. (London) **1**, 223 (1976).

[16] W. Kleemann, Int. J. Mod. Phys. B **7**, 2469 (1993), and references therein.

[17] D. A. Huse and D. S. Fisher, Phys. Rev. B **35**, 6841 (1987).

[18] R. Wang and M. Itoh (unpublished).